Int. J. Electrochem. Sci., 14 **(2019)** 6586 – 6602, doi: 10.20964/2019.07.38

International Journal of
ELECTROCHEMICAL
SCIENCE
www.electrochemsci.org

Effect of Methoxypolyethylene Glycol on Trivalent Chromium Electrodeposition

Wenjuan Zhang[1], *Lei Shi*[1], *Dongfang Niu*[1], *Heng Xu*[2], *Xinsheng Zhang*[1,*] *and Shuozhen Hu*[1,*]

[1] State Key Laboratory of Chemical Engineering, East China University of Science and Technology, Shanghai, 200237, China
[2] Collaborative Innovation Center for Petrochemical New Materials, Anqing, 246011, Anhui, China
[*]E-mail: shuozhen.hu@ecust.edu.cn, xszhang@ecust.edu.cn

Received: 18 March 2019 / *Accepted:* 6 May 2019 / *Published:* 10 June 2019

The effect of methoxypolyethylene glycol (mPEG) on chromium electrodeposition from a mixture of 1-butyl-3-methylimidazolium-bromide ([BMIM]Br) ionic liquid and water is studied. The addition of mPEG does not affect the two-step reduction process of Cr(III). With the presence of mPEG in the electrolyte, the diffusion coefficient decreases dramatically, and the resistance of the electrolyte and charge transfer increase, resulting in a reduced deposition rate and a smooth and crack-free coating surface. The hydrogen evolution reaction is suppressed, and more metallic Cr is deposited in the coating layer. Considering both the surface morphology and corrosion resistance, 80 mmol L^{-1} mPEG is the optimum concentration for smooth and pinhole-free chromium electrodeposition in the mixture of [BMIM]Br ionic liquid and water.

Keywords: Trivalent chromium, Electrodeposition, 1-Butyl-3-methylimidazolium-bromide ionic liquid, Methoxypolyethylene glycol

1. INTRODUCTION

The electrodeposition of chromium is widely used in the electronics, aerospace, automotive, and mechanical industries since chromium coatings have good corrosion and wear resistance, thermal stability, and unique optical properties [1-2]. Hexavalent chromium (Cr(VI)) aqueous electrolytes are commonly used for chromium electrodeposition. However, the utilization of Cr(VI) is restricted in many applications since Cr(VI) is highly toxic and can cause serious environmental and health problems [3]. Compared to Cr(VI), trivalent chromium (Cr(III)) is much less toxic [4-5]. Cr(III) is the most promising alternative chromium source. Unfortunately, trivalent chromium ions are surrounded by water molecules in aqueous electrolytes, easily forming a stable octahedral hexaaquachromium(III) complex

($[Cr(H_2O)_6]^{3+}$) [6]. The electrochemical reduction of Cr(III) can only proceed at a potential that is more negative than that required for the reduction of water [7]. Consequently, hydrogen is produced, which decreases the current efficiency for Cr(III) reduction. Furthermore, with the production of water, the pH value increases near the substrate surface [8], resulting in olation: a layer of polyoxides forms on the substrate surface, and chromium hydroxide ($Cr(OH)_3$) is precipitated [9-10]. These problems severely impede the reduction of trivalent chromium in aqueous solutions.

Ionic liquids, as an emerging kind of alternative electrolyte, feature high ionic conductivity, a wide electrochemical window, and low volatility and have attracted tremendous interest in many applications [11-12]. Electrolytes consisting of ionic liquids without water can fundamentally prevent the formation of hexaaquachromium(III) complexes and the hydrogen evolution reaction. He et al. [13] used anhydrous $CrCl_3$ to deposit Cr in 1-butyl-3-methylimidazolium bromide ([BMIM]Br) and formed dense and crack-free coatings. However, to maintain a water-free system, the experiments must be performed in a glove box, and anhydrous $CrCl_3$ needs to be used, which is expensive and difficult to obtain and maintain. In addition, anhydrous chromium salts have poor solubility in ionic liquids. The solubility of $CrCl_3$ in $[BMIM][BF_4]$ is only 0.4 mol L^{-1}. To simplify experiments and improve solubility, chromium(III) chloride hexahydrate ($CrCl_3 \cdot 6H_2O$), which is the most common Cr(III) salt, was used by Joan F. Brennecke and coworker [14]. The authors electrodeposited chromium in different imidazolium chloride ionic liquids with the addition of a certain amount of water. Although the Cr coatings exhibited good adherence to the substrate with a thickness of approximately 30.51 μm in [BMIM]Cl-based mixtures, the coating surface was full of holes and cracks, which resulted from the HER from water molecules. Similar results were also found earlier by S. Eugénio et al. [15]. The authors electrodeposited black chromium (Cr_2O_3) from $CrCl_3 \cdot 6H_2O$ in 1-butyl-3-methylimidazolium tetrafluoroborate $[BMIM][BF_4]$ ionic liquid. The chromium layer consisted of chromium nanoparticles with a size of approximately 17 nm. Based on their results, $[BMIM]^+$-based ionic liquid is a good candidate for chromium electrodeposition. Nevertheless, the formation of Cr_2O_3 nanoparticles, holes, and cracks on the coating surface are all because of the hydrogen evolution reaction. Thus, it is necessary to add some additives to prevent the HER effect in electrolytes containing both ionic liquids and water.

Polyethylene glycol (PEG) and its derivatives are the most common additives in metal electroplating. In particular, for copper electrodeposition, PEG is used as the inhibitor. With the addition of PEG, Cu-PEG-Cl complexes are formed on the electrode surface, which reduces the nucleation rate and the Cu^{2+} deposition rate [16]. As a result, a smooth copper layer is deposited. PEG has also been used as an additive for chromium electrodeposition in aqueous electrolytes [17]. PEG can adsorb on the electrode surface and prevent the hydrogen evolution reaction. Lee et al. [18] used PEG for chromium electrodeposition in aqueous solution and proved that PEG molecules are stable and decrease the reduction current of HER during electrodeposition. However, PEG and its derivatives have not been used for chromium deposition in ionic liquids.

In this study, the effect of methoxypolyethylene glycol (mPEG) on chromium electroplating in a mixture of 1-butyl-3-methylimidazolium-bromide ([BMIM]Br) ionic liquid and water was studied. Different amounts of mPEG were used as the additive. The electrodeposition mechanism of chromium in all $CrCl_3$/[BMIM]Br/H_2O and mPEG/$CrCl_3$/[BMIM]Br/H_2O electrolytes was studied by cyclic voltammetry (CV) experiments. The function of mPEG was studied by UV-vis, linear sweep

voltammetry (LSV), electrochemical impedance spectroscopy (EIS), and chronocoulometric (CC) measurements. X-ray diffraction (XRD), X-ray photoelectron spectroscopy (XPS), energy-dispersive X-ray spectroscopy (EDS), and scanning electron microscopy (SEM) were utilized to analyse the chemical state, elemental composition, and morphology. Polarization curves were obtained to analyse the coating corrosion resistance. The chromium coating electrodeposited from a mPEG/$CrCl_3$/[BMIM]Br/H_2O bath with 80 mmol L^{-1} mPEG exhibited the best surface morphology and corrosion resistance.

2. EXPERIMENTAL SECTION

2.1. Ionic liquid synthesis

1-Butyl-3-methylimidazolium-bromide ([BMIM]Br) ionic liquid was synthesized and purified according to the literature [19]. First, 1 mol of N-methyl imidazole (Analytical Reagent, Aladdin) was heated in a round-bottom flask with reflux condensation. When the temperature reached 60 °C, 1.1 mol of 1-butyl bromide (Analytical Reagent, Aladdin) was added dropwise to the flask. Then, the temperature was maintained at 80 °C for three hours after adding the 1-butyl bromide. When the temperature of the mixture cooled to 60 °C, acetone and [BMIM]Br seed solution were added and stirred until all the synthesized [BMIM]Br precipitated. The solid was filtered when it was warm and washed with acetone until the filtrate was clear and colourless. Finally, the white [BMIM]Br solid was vacuum dried at 80 °C for 24 hours.

2.2. Electrolyte preparation

A total of 6.72 g of chromium chloride ($CrCl_3 \cdot 6H_2O$) (Analytical Reagent 98%, Aladdin) and 2.73 g of Millipore® water (18.3 MΩ) were added to 10 mL of [BMIM]Br ionic liquid to obtain $CrCl_3$/[BMIM]Br/H_2O electrolyte with a molar ratio of 1:2:12. The electrolyte was stirred for 24 hours at 40 °C to ensure that the chromium salt was completely dissolved. To study the methoxypolyethylene glycol (mPEG) effect, a certain amount of mPEG (PEG-350-MME solution, Macklin) was added to the $CrCl_3$/[BMIM]Br/H_2O solution to obtain electrolytes with 40, 60, 80, and 100 mmol L^{-1} mPEG.

The electrolytes containing mPEG, $CrCl_3$, [BMIM]Br, and H_2O (i.e. mPEG/$CrCl_3$/[BMIM]Br/H_2O) are named as Br-mPEG in general. For the electrolytes with exact amount of mPEG, the concentration of mPEG is added after "Br-mPEG". For example, the electrolyte with 40 mmol L^{-1} of mPEG is named as Br-mPEG40. The electrolytes with 60 mmol L^{-1}, 80 mmol L^{-1}, and 100 mmol L^{-1} of mPEG are named as Br-mPEG60, Br-mPEG80, and Br-mPEG100, respectively. The electrolyte without mPEG (i.e. $CrCl_3$/[BMIM]Br/H_2O) is named as Br-mPEG0.

2.3. Electrochemical measurements.

A CHI602E electrochemical workstation was applied for electrochemical measurements of chromium electrodeposition. A three-electrode configuration was used with a glassy carbon electrode

($0.07\ cm^2$) as the working electrode, a platinum mesh (0.5 cm × 1.5 cm) as the counter-electrode, and a platinum wire as the reference electrode. The electrolyte temperature was maintained at 40 °C during the whole experiment. Before each electrochemical measurement, the working electrode was mechanically polished with 0.05 mm alumina slurries on lapping pads. Then, the electrode was rinsed with Millipore® water (18.3 MΩ) and dried in air. Cyclic voltammetry (CV) was performed in [BMIM]Br/H_2O, Br-mPEG0 and Br-mPEG80 electrolytes at a scan rate of 50 mV s^{-1}. To obtain the diffusion coefficient, CVs in all Br-mPEG0 and Br-mPEG electrolytes were performed at different scan rates ranging from 10 to 60 mV s^{-1} with 10 mV intervals. Electrochemical impedance spectroscopy (EIS) was performed by an Autolab workstation (PGSTAT 302N) in Br-mPEG electrolyte with different mPEG concentrations at -1.4 V (vs. Pt) with a frequency range from 10^{-2} to 10^5 Hz at an AC amplitude of 5 mV. Chronocoulometry (CC) was measured in Br-mPEG electrolyte with different mPEG concentrations at -1.0 V (vs. Pt).

2.4. Electrodeposition

Chromium electrodeposition was performed with a CHI602E electrochemical workstation. A platinum mesh (0.5 cm × 1.5 cm) was used as the anode, and a piece of brass foil (10 mm × 10 mm, 99.9%) was used as the cathode. The non-working area was coated with a piece of insulating tape. The electrolyte was stirred continuously at 40 °C during the electrodeposition process. The distance between the cathode and anode was maintained at 1 cm. Electrodeposition was performed for one hour at -3.0 V. All the glassware used in the experiments was cleaned with 0.2 mol L^{-1} chromic acid solution and Millipore® water (18.3 MΩ) successively. Before deposition, the brass foil was polished with rough and fine sandpaper successively to remove any oxide layer formed on the surface. Then, the polished brass foil was sonicated in 0.25 mol L^{-1} NaOH ethanol solution, 0.1 mol L^{-1} HCl, and dehydrated ethanol successively. Finally, the cleaned brass foil was dried. After electrodeposition, the samples were washed in ethanol to remove the [BMIM]Br residue and then dried with cold air and separately kept in sealed vials.

2.5. Physical measurements

The UV-vis spectra of the electrolytes were taken immediately after the total dissolution of $CrCl_3 \cdot 6H_2O$ in a mixture of [BMIM]Br, water, and mPEG by using an Agilent 8453 UV spectrophotometer with an integrating sphere detector at room temperature. Scanning electron microscopy (SEM) was used to detect the microstructure and surface morphology of the Cr coatings by using a Nova NanoSEM 450. The crystalline structures of the Cr coatings were examined by X-ray diffraction (XRD) with a Bruker AXS D8 Advance using a Cu Kα radiation source (λ = 0.15405 nm) over a scanning range from 20° to 80°. The bulk concentrations of Cr, O, and Cl in the coatings were assessed with energy-dispersive X-ray spectroscopy (EDS) by using an EDAX Falion 60S. The surface components and oxidation state of the deposited Cr layers were investigated by X-ray photoelectron

spectrometry (XPS), which was measured by using a ThermoFisher ESCALAB 250Xi with an Al K_α X-ray source (1486.6 eV) and calibrated against C 1s at 284.6 eV.

3. RESULTS AND DISCUSSION

3.1. Study of the reduction mechanism of Cr^{3+}

Cyclic voltammetry (CV) is one of the most useful techniques to test the electrochemical stability of electrolytes and the reaction mechanism of reactants. In the CV results for a mixture of [BMIM]Br ionic liquid and water ([BMIM]Br/H_2O) (shown in Fig. 1), there is a reduction peak at ca. -0.3 V and an oxidation peak at ca. 0.3 V, which can be attributed to the redox of bromine ions. As the potential continues to decrease, a cathodic current appears at approximately -2.3 V, indicating that the $[BMIM]^+$ cations are reduced to carbenes [20] or that the hydrogen evolution reaction (HER) starts. This result indicates that [BMIM]Br/H_2O is electrochemically stable in the potential range between 0.4 and -2.3 V and has an electrochemical window of approximately 2.7 V, which is approximately consistent with the literature results [13]. Two new peaks are observed at -1.48 V and -2.1 V with Br-mPEG0 electrolyte, as shown in Fig. 1. These two peaks suggest that the reduction of Cr(III) in [BMIM]Br/H_2O electrolyte proceeds a two-step mechanism via Cr(II). Peak A (at -1.48 V) is attributed to the reduction of Cr(III) to Cr(II) (Equation 1). Peak B (at -2.1 V) indicates the further reduction of Cr(II) to metallic chromium (Equation 2). This result agrees with the normally accepted mechanism for Cr(III) reduction in both ionic liquids [12] and aqueous liquids [21,22].

$$Cr^{3+} + e^- \rightarrow Cr^{2+} \quad (1)$$

$$Cr^{2+} + 2e^- \rightarrow Cr^0 \quad (2)$$

The CV results of Br-mPEG80 electrolyte is also illustrated in Fig. 1. Two reduction peaks for Cr(III) are also observed with mPEG, indicating that the addition of mPEG does not affect the two-step mechanism of chromium reduction. However, the current decrease for all the peaks indicates that chromium electrodeposition is limited by mPEG.

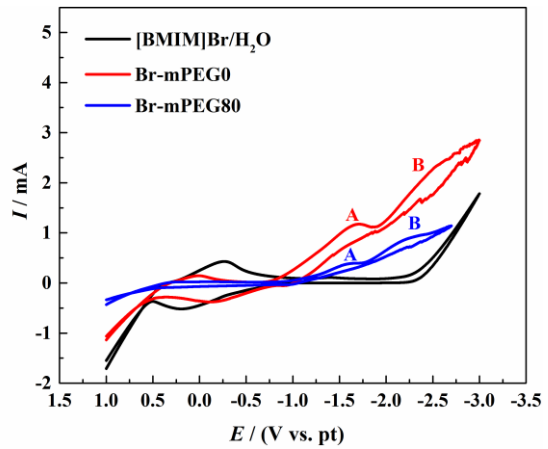

Figure 1. Cyclic voltammograms of [BMIM]Br/H_2O, Br-mPEG0 and Br-mPEG80 electrolytes on a GC electrode at 40 °C at a scan rate of 50 mV s^{-1}.

3.2. mPEG effect

3.2.1. Chromium complex structure

It is well known that chromium ions are present in the form of hexaaquachromium(III) ions ($[Cr(H_2O)_6]^{3+}$) in aqueous baths [23-24]; these ions are present in a stable octahedral structure and difficult to decompose. Depending on the concentration of chloride ions in the solution, there is a dynamic balance between Cr(III) and the ligands, i.e., Cl^- and H_2O, in the chromium complex structure (Equation 3).

$$[Cr(H_2O)_6]Cl_3 \leftrightarrow [Cr(H_2O)_5Cl]Cl_2 \cdot H_2O \leftrightarrow [Cr(H_2O)_4Cl_2]Cl \cdot 2H_2O \leftrightarrow [Cr(H_2O)_3Cl_3] \cdot 3H_2O \quad (3)$$

Consequently, the potential required to reduce Cr(III) from different complexes varies. Thus, it is important to detect the complex structure in the electrolyte to determine the reduction ability. UV-vis analysis was used to detect complex formation. In this study, two broad absorption bands with maxima at approximately 480 nm and 680 nm were observed (shown in Fig. 2), which can be attributed to the transition of $4A_{2g}$ to $4T_{2g}$ and $4A_{2g}$ to $4T_{1g}$, respectively [25]. According to Brennecke [14], the predominant chromium complex structure is $[Cr(H_2O)_4Cl_2]^+$ in Br-mPEG0 (Cr:[BMIM]:H_2O = 1:2:12, molar ratio) electrolyte. As the molar ratio between Cr(III), $[BMIM]^+$, and H_2O used in this study is the same as that used in Brennecke's research, it is speculated that $[Cr(H_2O)_4X_2]^+$ is also the main complex in this study. However, a redshift in the absorption spectra was detected (484 nm and 680 nm) compared to the results for $[Cr(H_2O)_4Cl_2]^+$ in a Br-mPEG0 bath from Brennecke's research (452 nm and 631 nm). This could be because bromine ions (Br^-) are the anions in this study instead of Cl^-. The Cl^- from chromium salt could be replaced by Br^-. Thus, the ligand X in $[Cr(H_2O)_4X_2]^+$ could be Br^- or a mix of Br^- and Cl^-. Since UV-vis absorption bands are sensitive to the chromium surroundings and ligands, Br^- replacement could be the reason for the redshift.

In the electrolytes containing mPEG, both the upper and lower bands are slightly blue shifted without a change in band shape compared to the results for the Br-mPEG0 (shown in Fig. 2). According to Brennecke [14] and Elving [26], a blueshift suggests that the amount of H_2O molecules in the chromium complex is increased in either the ionic liquid or aqueous solution. In this study, since mPEG contains hydrophilic functional groups, these groups could attract the H_2O molecules in the chromium complex and slightly increase the distance between the H_2O molecules and Cr^{3+}. Consequently, a small amount of water from the electrolyte could be attracted to the chromium complex, resulting in a blueshift in the UV-vis bands. However, since the blueshift in the bands obtained from UV-vis is minor compared to those obtained by Brennecke (from 464.5 to 441.5 nm) [14], the change in the amount of H_2O molecules in the chromium complex is negligible.

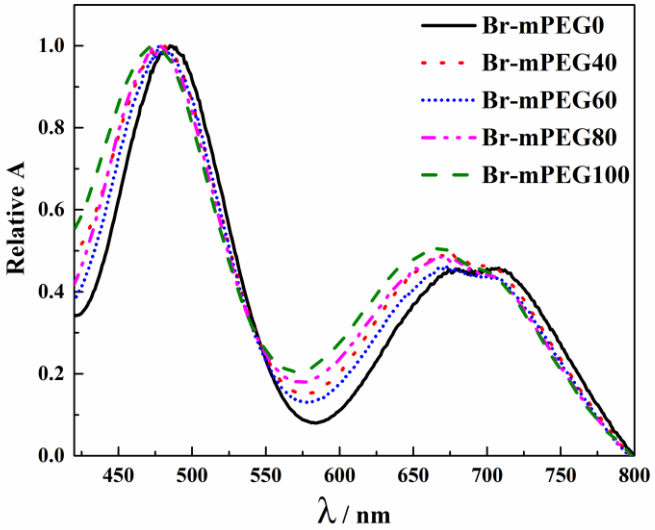

Figure 2. UV–vis spectra of Br-mPEG electrolyte containing various concentrations of mPEG.

3.2.2. Chromium electrodeposition diffusion coefficient

A series of cyclic voltammetry experiments with different scan rates from 10 $mV{\cdot}s^{-1}$ to 60 $mV{\cdot}s^{-1}$ [13] were performed to study the deposition kinetics in more detail and to determine the diffusion coefficient of Cr(III) in Br-mPEG0 electrolyte and Br-mPEG electrolyte. As Fig. 3a shows, a small anodic peak was detected at approximately -1.1 V for all the CV results in Br-mPEG0 electrolytes, which suggest that some Cr(II) can be oxidized back to Cr(III) during the anodic scan, indicating that the reduction of Cr(III) to Cr(II) is a quasi-reversible process in Br-mPEG0 electrolyte. However, this anodic peak was significantly reduced with the presence of mPEG in the electrolyte (see Fig. 3b), suggesting the irreversible reaction of Cr(III) with mPEG. Moreover, Fig. 3b shows a negative shift in the cathodic peak potential and an increase in the cathodic peak current as the scan rate increases in Br-mPEG80 electrolyte. As a comparison, a series of CV experiments with different scan rates were also performed with Br-mPEG40 electrolyte, the results of which are not shown here. A linear relationship between the peak potential E_p and ln$v$ was also obtained for Br-mPEG40 and Br-mPEG80 (see Fig. 3c). This peak potential shift and linear relationship confirm the irreversible reduction of Cr(III) to Cr(II) in Br-mPEG electrolyte and indicates that mPEG can prevent the oxidation of Cr(II).

As Fig. 3d shows, a linear relationship was obtained between the cathodic peak current density (I_p) and $v^{1/2}$ electrolytes either with or without mPEG, indicating that the Cr(III) reduction process is diffusion controlled in both electrolytes. Since the reduction of Cr(III) to Cr(II) is an irreversible reaction, the relationship between I_p and $v^{1/2}$ follows Equation 4 [15].

$$I_p = \frac{0.282\pi^{\frac{1}{2}}F^{\frac{3}{2}}}{(RT)^{\frac{1}{2}}}\mathrm{n}(\alpha \mathrm{n}_\alpha)^{\frac{1}{2}}D^{\frac{1}{2}}C_0\nu^{\frac{1}{2}} \quad (4)$$

where v is the potential scan rate, n is the number of electrons transferred, D is the diffusion coefficient and C_0 is the Cr(III) concentration. The average value of αn_α can be obtained from Equation 5 for an irreversible reaction [27]:

$$\left|E_p - E_{\frac{p}{2}}\right| = \frac{1.875RT}{\alpha n_\alpha F} \quad (5)$$

where E_P is the peak potential, $E_{P/2}$ is the half-peak potential, T is the absolute temperature, R is the gas constant, F is the Faraday constant, n_α is the number of electrons transferred in the rate-determining step, which is one for Cr(III) to Cr(II), and α is the charge transfer coefficient. The diffusion coefficient of Cr(III) in Br-mPEG0 calculated by Equation (5) is 1.02 x 10^{-6} cm^2 s^{-1}, which is slightly lower than the diffusion coefficient obtained for [BMIM]Br by He et al. (2.3 × 10^{-6} cm^2 s^{-1}) since the operation temperature was 40 °C lower in this study [13]. The diffusion coefficient for Cr(III) was dramatically decreased by one order of magnitude to 1.04 x 10^{-7} cm^2 s^{-1} after adding 40 mmol L^{-1} mPEG in electrolyte. However, as the concentration of mPEG increased to 80 mmol L^{-1}, the diffusion coefficient of Cr(III) did not change much (1 × 10^{-7} cm^2 s^{-1}). This could be because the mPEG molecules are attracted to the chromium complex due to the interaction between the hydrophilic functional groups on mPEG and the water molecules in the chromium complex. The volume of the chromium complexes increases, so the diffusion coefficient of chromium ions decreases.

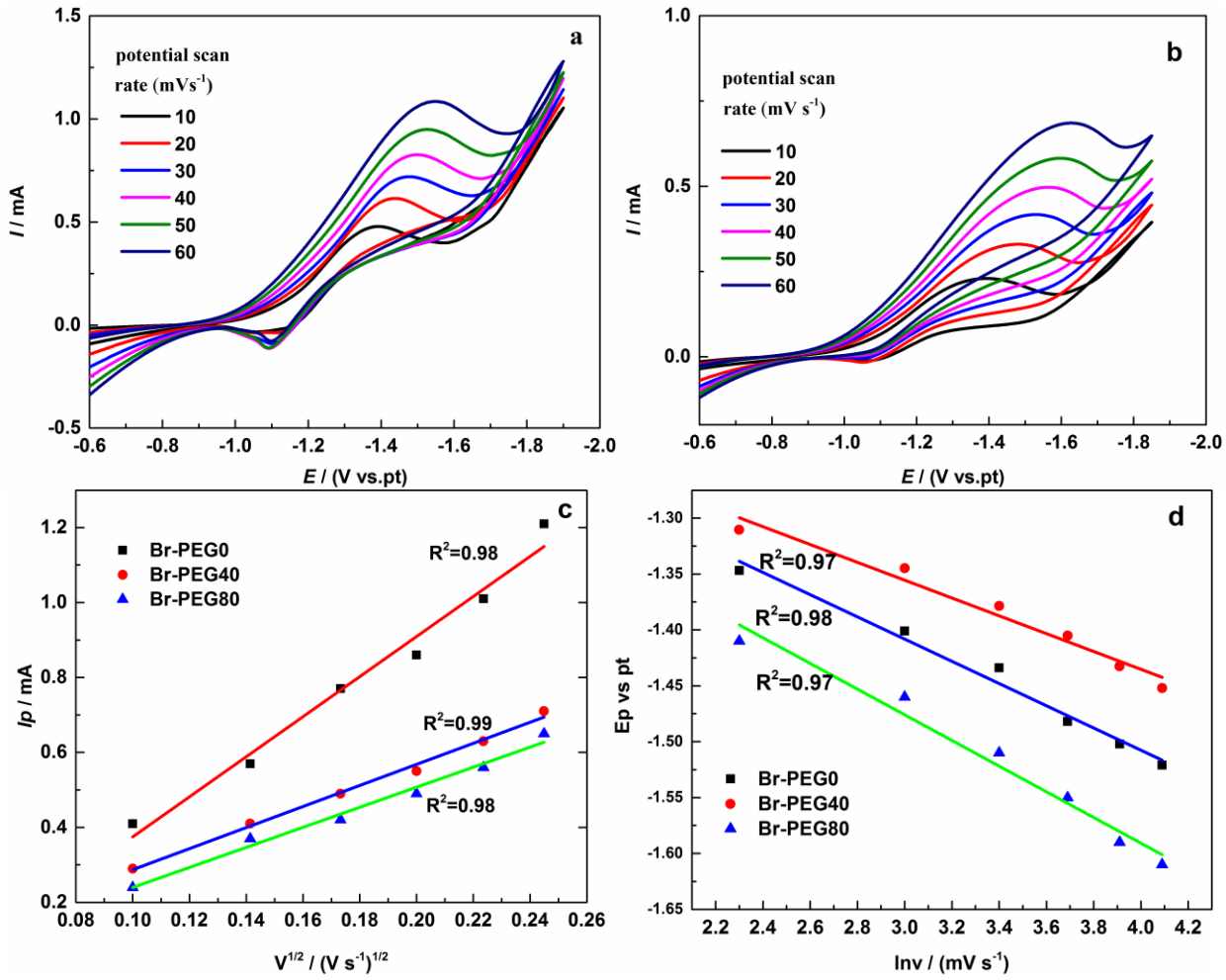

Figure 3. Cyclic voltammograms of Br-mPEG0 (a) and Br-mPEG80 (b) on a GC electrode at 40 °C with potential scan rates between 10 and 60 mV s^{-1}. The relationship between E_p and ln$v$ (c) and I_p and $v^{1/2}$ (d) for Cr(III) reduction in Br-mPEG0 and Br-mPEG solution.

3.2.3. Resistance and surface coverage

mPEG is a non-conductive polymer that not only affects the diffusion coefficient of Cr(III) but also can alter the resistance of the electrolyte. In addition, as a surface wetting agent, mPEG can adsorb on the electrode surface during the deposition process. Therefore, the charge transfer resistance and the concentration of Cr(III) adsorbed on the electrode surface before and after adding mPEG need to be studied. The effect of different concentrations of mPEG during Cr(III) electroplating was analysed in more detail by electrochemical impedance spectroscopy (EIS) and chronocoulometry (CC).

The EIS diagrams and the fitting results of Br-mPEG electrolytes with different concentrations of mPEG under a potential of -1.4 V at 40 °C are shown in Fig. 4a. The relevant electrochemical equivalent circuit is shown as the inset. The values of the equivalent circuit elements are listed in Table 1, where R_s and R_{ct} represent the resistance of the electrolyte and charge transfer, respectively. As shown in Fig. 4a, when the electrolyte is free of mPEG, R_s and R_{ct} are 0.66 kΩ and 0.70 kΩ, respectively. After the addition of mPEG, both R_s and R_{ct} increase as the concentration of mPEG increases. mPEG is a liquid with high viscosity. The addition of mPEG reduces the diffusion coefficient of chromium, thus reducing the electromobility of chromium ions and increasing the electrolyte resistance. The charge transfer resistance increases because of the adsorption of mPEG on the electrode surface.

Chronocoulometry (CC) was employed to determine the effect of mPEG on the surface coverage of Cr(III) in the five electrolytes studied in this research according to Equation 6[28-29].

$$Q = \frac{2nFACD^{\frac{1}{2}}}{\pi^{\frac{1}{2}}} t^{1/2} + Q_{dl} + nFA\Gamma^* \quad (6)$$

where D is the diffusion coefficient, A is the surface area of the electrode, Q_{dl} is the capacitive charge, $nFA\Gamma^*$ is the faradic component representing the change in surface coverage and Γ^* is the amount of adsorbed reactant (mol cm^{-2}). The corresponding CC curves obtained from various concentrations of mPEG are shown in Fig. 4b. Since chromium reduction is related to the coverage of Cr(III) on the substrate surface, it is important to obtain the Cr(III) amount adsorbed on the surface. Thus, -1.0 V (vs. Pt) was utilized as the applied potential to eliminate the charge collected from the reduction of Cr(II) and water. From the intercept of the plot of Q vs. $t^{1/2}$, the Cr(III) coverage was obtained and is listed in Table 1. The results clearly show that Cr(III) coverage does not change much when 40 mmol L^{-1} mPEG is in the electrolyte. According to copper electrodeposition, PEG molecules quickly adsorb on the electrode surface after being added to the electrolyte and reduce the Cu^{2+} coverage [30]. However, the Cr(III) coverage did not change much with 40 mmol L^{-1} mPEG in the electrolyte in this study. This might be because $[BMIM]^+$ ions and H_2O molecules are adsorbed on the electrode and block the active sites before adding mPEG. With the addition of mPEG molecules on the electrode surface, the C-O-C and -OH structures of mPEG attract H_2O molecules and remove them from the electrode surface. However, the active sites of the substrate are covered by mPEG instead. Overall, mPEG has a greater effect on reducing the adsorption amount of H_2O molecules, and the coverage of Cr(III) is not substantially affected when there is 40 mmol L^{-1} mPEG in the electrolyte. However, as the concentration of mPEG increases, more mPEG molecules adsorb on the electrode surface, which eventually affects the adsorption amount of Cr(III) ions.

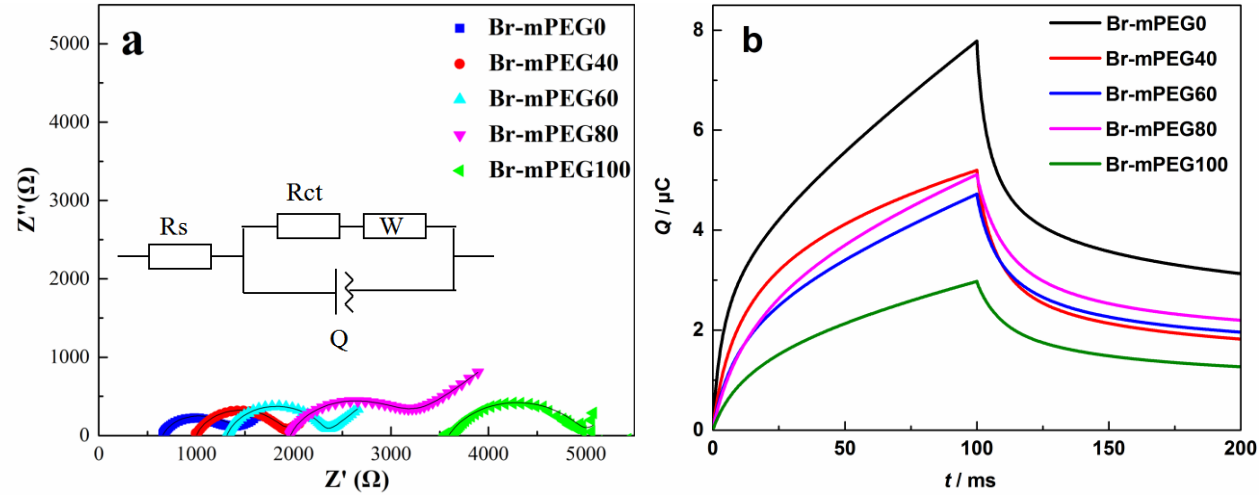

Figure 4. EIS (a) and chronocoulometry (b) results for Br-mPEG electrolytes containing various mPEG concentrations. The inset of (a) is the relevant electrochemical equivalent circuit.

Table 1. Values of the equivalent circuit elements fitted to the EIS results and the amount of adsorbed Cr(III) ions obtained by chronocoulometric measurements.

Sample	R_s / kΩ	R_{ct} / kΩ	Γ^* / mol cm^{-2}
Br-mPEG0	0.66	0.70	4.83E-06
Br-mPEG40	1.00	0.89	4.35E-06
Br-mPEG60	1.32	1.01	3.96E-06
Br-mPEG80	1.97	1.20	3.85E-06
Br-mPEG100	3.59	1.39	2.13E-06

3.2.4. Linear sweep voltammetry

It is well known that the chromium deposition current efficiency is low since there is competition between the HER and the Cr(II) reduction reaction in electrolytes containing water. More importantly, OH^- is produced during the HER, which can react with Cr(III) ions to form $Cr(OH)_3$ to reduce the Cr coating quality. Thus, it is necessary to limit the HER during chromium deposition to improve the current efficiency and Cr coating quality. With mPEG in the electrolyte, as Fig. 5a shows, the hydrogen evolution onset potential is more negative when 60 mmol L^{-1} mPEG is added to the electrolyte. The onset potential is related to the concentration of H_2O molecules on the electrode surface, according to the Nernst equation. Because glassy carbon was utilized for all the LSV experiments, the standard redox potential should not be affected. Therefore, the negative shift in onset potential is a result of lowering the concentration of *Ox* species, which is H_2O here. Thus, with the addition of mPEG, the amount of H_2O molecules adsorbed on the surface is significantly reduced, which agrees with the CC results. As shown in Fig. 5a, the current for the HER also decreases, meaning that the reducing rate of H_2O is decreased. One of the reasons is that the diffusion coefficient is reduced in the presence of mPEG. In addition, as the EIS results demonstrate, both the electrolyte resistance and the charge transfer resistance are

increased when the electrolyte contains 60 mmol L^{-1} mPEG. Thus, mPEG has an obvious inhibitory effect on the hydrogen evolution reaction, which agrees with the literature results for PEG in the aqueous phase [18].

To study the effect of mPEG on the chromium electrochemical reduction reaction in more detail, linear sweep voltammetry (LSV) was utilized at a scan rate of 20 mV s^{-1}. As Fig. 5b shows, in the mPEG-free electrolyte, a reduction peak is obtained at approximately -1.3 V, which belongs to the reduction of Cr(III) to Cr(II). A broad bump between -1.7 V and -2.2 V is obtained for Cr(II) reduction to Cr metal. As the potential continues to decrease below -2.2 V, the current begins to fluctuate because the hydrogen bubbles are produced from the hydrogen evolution reaction (HER). With 40 mmol L^{-1} mPEG in the electrolyte, there is a significant current decrease for all peaks. However, the onset potential of Cr(III) reduction to Cr(II) does not change obviously. The current decrease indicates that the chromium reduction rate is reduced as a result of the electrolyte resistance increase. Moreover, the diffusion coefficient of Cr(III) in the electrolyte with 40 mol L^{-1} mPEG is dramatically reduced, which also contributes to the lower current. Although mPEG molecules adsorb on the electrode surface quickly, the surface coverage of Cr(III) on the electrode surface does not change much. Thus, the onset potential of Cr reduction does not shift according to the Nernst equation. As the mPEG concentration increases, more mPEG molecules adsorb on the electrode and remain in the electrolyte. The coverage of Cr^{3+} on the electrode surface decreases (listed in Table 1).

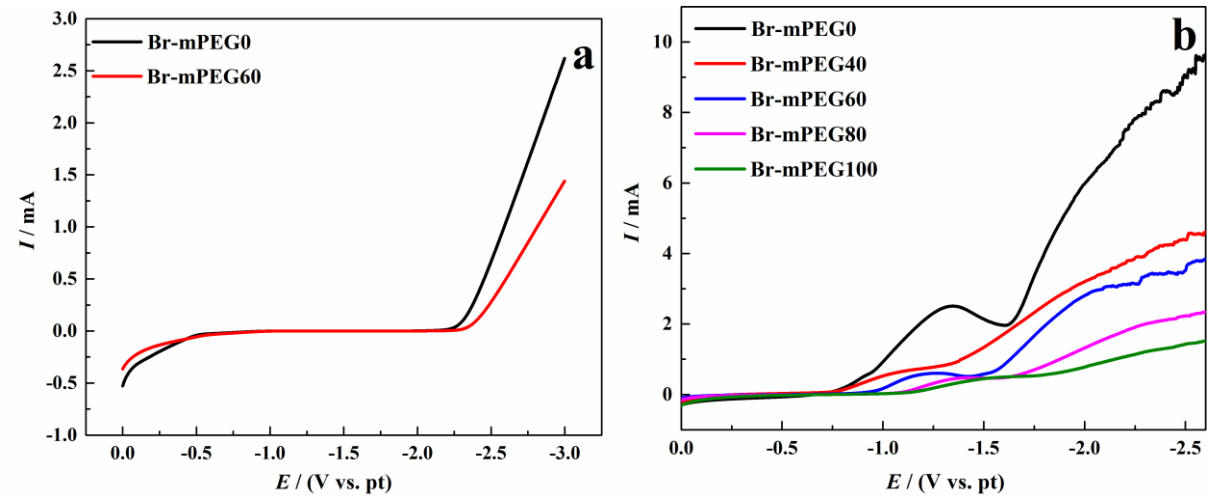

Figure 5. LSV of the hydrogen evolution reaction in [BMIM]Br/H_2O electrolytes with and without mPEG (a) and chromium reduction in Br-mPEG with different mPEG concentrations (b) at a scan rate of 20 mV s^{-1}.

Consequently, chromium reduction and the HER are further hindered, resulting in a negative shift in the onset potential of Cr(III) reduction and lowering the current. When there is 100 mmol L^{-1} mPEG in the electrolyte, the onset reduction potential does not decrease much compared to that for Br-mPEG80, suggesting that the electrode is almost covered by a whole layer of mPEG. In summary, mPEG can simultaneously suppress both the hydrogen evolution reaction and chromium electroplating in decreasing the diffusion and reduction processes. With 40 mmol L^{-1} mPEG in the electrolyte, the

suppression effect is more significant for the HER. In addition, according to the UV-vis results, the presence of a large amount of mPEG molecules can also increase the number of water molecules in the chromium complex, which also makes chromium electrodeposition more difficult and results in a more negative onset potential.

3.3. Surface morphology, composition, and structure of the chromium coatings

3.3.1. Morphological properties

To test the effect of mPEG on Cr coating morphology, chromium was electrodeposited in electrolytes with different amounts of mPEG. Fig. 6a-f present SEM images of Cr coatings electroplated for one hour in Br-mPEG electrolyte containing 0 to 100 mmol L^{-1} mPEG. The electrodeposited chromium coating in Br-mPEG0 (Fig. 6a) has large particles and microcracks. Rough and uneven surfaces appear in the coating. The addition of mPEG to the trivalent chromium electrolyte significantly reduced the surface roughness (shown in Fig. 6b-d). This is because as more mPEG molecules are present in the electrolyte, the diffusion coefficient and the Cr(III) coverage are decreased, and the electrolyte resistance and charge transfer resistance are increased, which inhibits the reduction of chromium and decreases the chromium electrodeposition rate [31-32]. In addition, according to Lu et al., the surface stress is relieved by the introduction of cracks at a high diffusion rate, while at a low diffusion rate, the coating obtained is relatively flat [33].

However, pinholes are detected when the mPEG concentration increases to 100 mmol L^{-1} (shown in the inset of Fig. 6f), which does not occur for the electrolytes with mPEG concentrations between 40 and 80 mmol L^{-1}. When there is 100 mmol L^{-1} mPEG in the electrolyte, a thick layer of mPEG covers the electrode surface. Although the addition of mPEG can inhibit the HER, hydrogen bubbles can still be produced on the electrode. This thick layer of mPEG not only prevents the electrodeposition of chromium ions and the HER but also prevents the rapid diffusion of hydrogen bubbles from the coating surface to the bulk solution. Thus, pinhole defects are formed on the coating surface.

The thickness of the chromium coating was also measured. As Fig. 6g shows, the Cr coating thickness increases significantly after adding 40 mmol L^{-1} mPEG to the electrolyte. As explained earlier, even though the diffusion coefficient decreases and electrolyte resistance increases with 40 mmol L^{-1} mPEG in the electrolyte, the Cr(III) coverage on the surface is not significantly affected. According to the CC and LSV results, the HER is significantly suppressed with the addition of mPEG. Thus, the adsorption of mPEG on the electrode surface affects the HER more than Cr electrodeposition. During the chromium electrodeposition reaction, HER is the competing reaction. Consequently, the addition of 40 mmol L^{-1} mPEG resulted in a greater deposition of chromium. Alternatively, it can be concluded that the chromium electrodepositing current efficiency increased. However, with the further addition of mPEG to the electrolyte, chromium electrodeposition is prevented. Consequently, the thickness of the chromium coating decreases as the mPEG concentration increases.

Typical polarization curves of the Cr coatings were obtained in 1 mol L^{-1} HCl solution and are presented in Fig. 6h. The corrosion potential of the Cr coatings shifts to more positive values compared to that of a pure brass substrate. This result indicates that the Cr coatings enhanced the prevention of

corrosion due to the corrosion-resistance property of Cr coatings. Moreover, with increasing mPEG concentration, the polarization curves moved to higher potentials, except for that of Br-mPEG100.

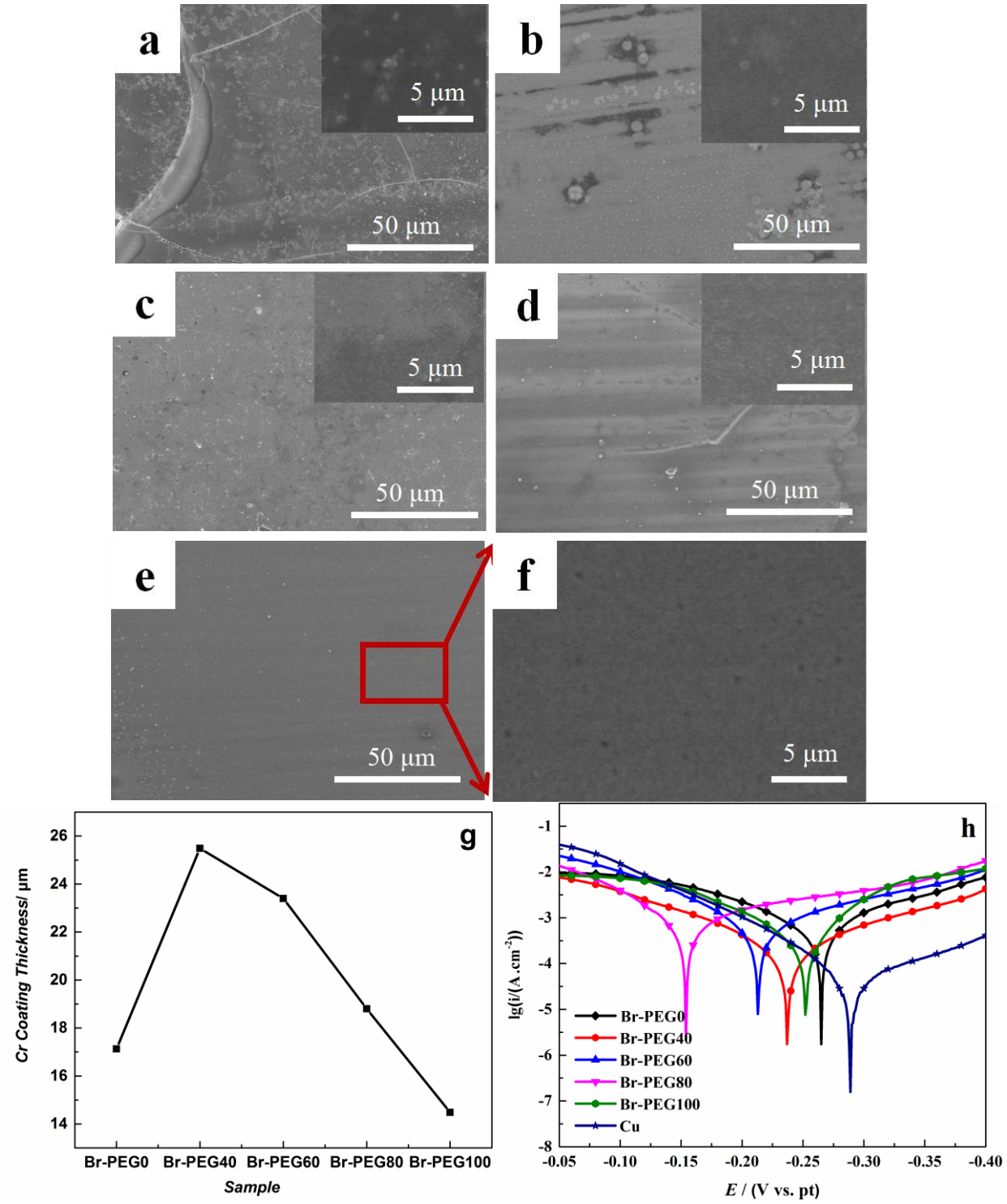

Figure 6. SEM images of chromium coatings obtained with Br-mPEG0 (a), Br-mPEG40 (b), Br-mPEG60 (c), Br-mPEG80 (d), Br-mPEG100 (e) and Br-mPEG100 (zoomed-in image) (f). The inset images in a, b, c, and d are zoomed-in images of each coating. Thickness of the chromium coatings (g) obtained from the five electrolytes at 0.1 A for 1 hour at 40 °C. Typical polarization curves (h) of chromium coatings obtained at -3.0 V in 1 mol L^{-1} HCl.

As Fig. 6a shows, cracks and rough surfaces with many small particles of chromium aggregates are present in the coatings without mPEG. This behaviour leads to poor corrosion resistance. With increasing mPEG content, the corrosion resistance is significantly improved. As Fig. 4a shows, the charge transfer resistance increases as the concentration of mPEG increases in the electrolyte. Consequently, the deposition rate decreases and the compactness of the coating increases because the coating tends to be smooth and free of cracks.

However, when the content of mPEG reaches 100 mmol L^{-1}, a large number of pinholes appear on the coating surface (shown in Fig. 6f), resulting in a decreased binding force between the coating and the substrate and poor corrosion resistance. Considering both the corrosion resistance and coating surface smoothness, the most suitable concentration of mPEG is 80 mmol L^{-1}. Thus, this concentration of mPEG during the electrodeposition of chromium is expected to be widely used in corrosion protection.

3.3.2. Composition of the chromium coatings

The surface composition of a coating can be obtained from X-ray photoelectron spectroscopy (XPS). Since the Br-mPEG80 sample has the best morphology and corrosion resistance among the coating samples prepared in this study, the core-level binding energies of Cr $2p_{3/2}$ for the Cr coatings deposited from the Br-mPEG0 and Br-mPEG80 electrolytes are shown in Fig. 7a. The deconvolution of the Cr $2p_{3/2}$ peaks shows three peaks at 574.65, 576.52 and 577.75 eV, representing metallic Cr, Cr_2O_3, and $Cr(OH)_3$, respectively, for both samples [34]. The amount of metallic Cr in the coating with Br-mPEG80 is approximately 1.8 times greater than that in the Br-mPEG0 coating. Detailed concentrations are listed in Table 2. This result confirms that with mPEG in the electrolyte, less OH^- is produced from the HER, resulting in more metallic Cr in the coating.

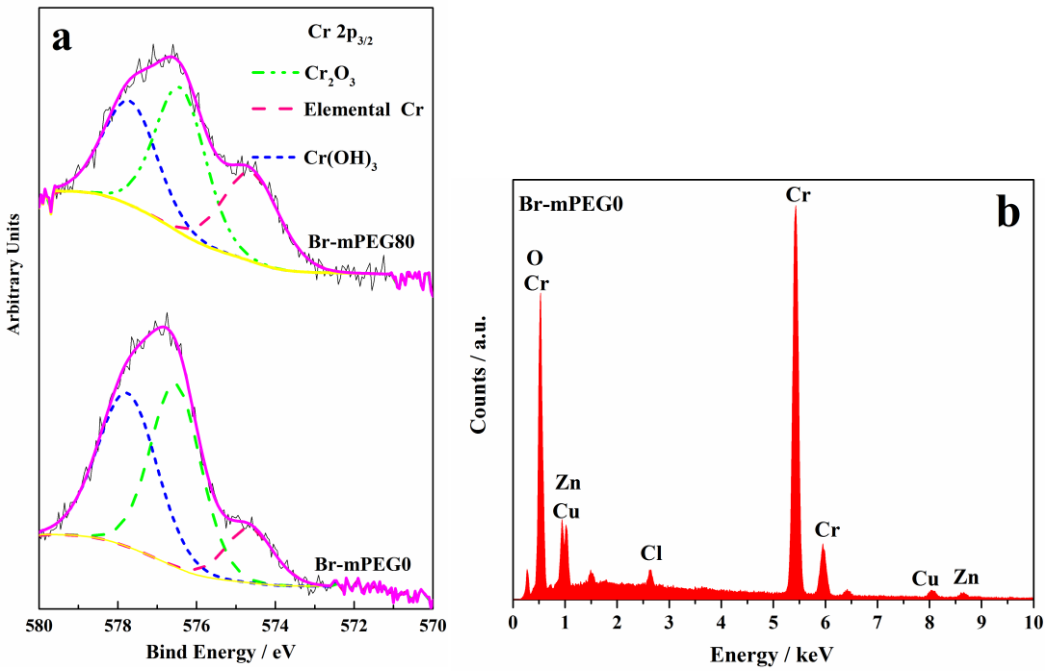

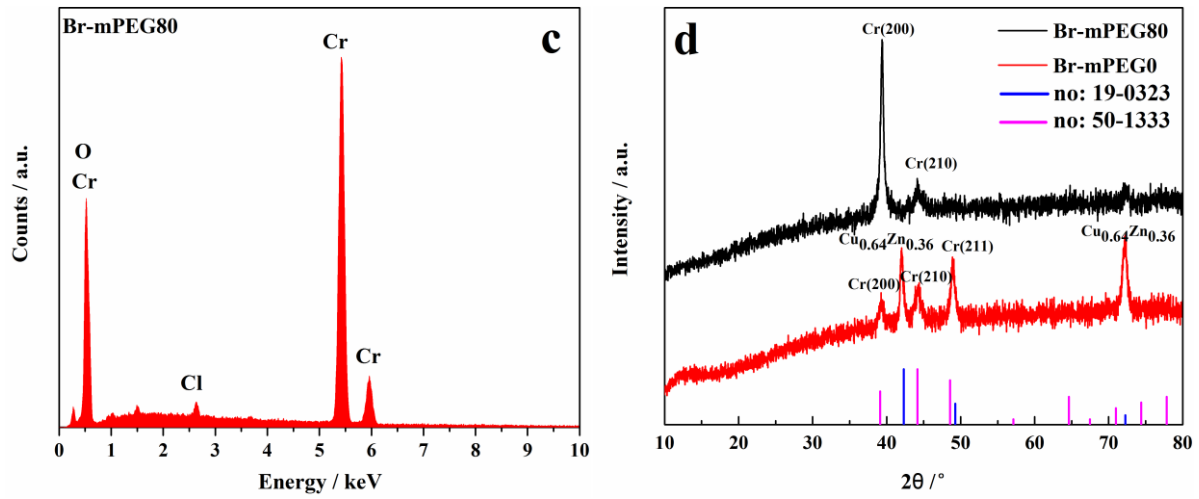

Figure 7. XPS Cr $2p_{3/2}$ spectra (a), EDS characterization (b) and (c), and XRD spectra (d) of the chromium coating deposited from Br-mPEG0 and Br-mPEG80 electrolytes.

Table 2. Surface composition of chromium coatings from Br-mPEG0 and Br-mPEG80 by XPS.

Sample	Composition (at.%)		
	Cr	Cr_2O_3	$Cr(OH)_3$
Br-mPEG0	14.12	43.03	42.86
Br-mPEG0	25.88	44.52	29.6

Table 3. Bulk composition of coatings from Br-mPEG0 and Br-mPEG80 by EDS.

Element	Br-mPEG0		Br-mPEG80	
	Chemical composition (%)		Chemical composition (%)	
	(by mass)	(by atomic content)	(by mass)	(by atomic content)
Cr	83.99	71.3	91.9	80.05
O	8.56	23.01	6.75	18.44
Cl	1.38	1.51	1.35	1.51
Cu and Zn	6.07	4.18	0	0

Since XPS is a surface technique to detect coating properties within the uppermost 10 nm thickness, the bulk concentration of the coating layer is detected by EDS. Fig. 7b presents clear Cr and O peaks. Based on the calculated peak area, the molar ratio of Cr:O is 3:1 and 4.4:1 for the coatings obtained from Br-mPEG0 and Br-mPEG80, respectively. Detailed values are listed in Table 3. Thus, mPEG has a substantial inhibitory effect on the HER and produces more metallic Cr. Small amounts of chloride are detected for both coatings, as $CrCl_3 \cdot 6H_2O$ was used as the precursor. Since the Br-mPEG0 coating has an uneven and cracked surface, the brass substrate is detected. However, this does not occur for the coating obtained from Br-mPEG80. This result also suggests that the surface morphology is improved with mPEG in the electrolyte.

The XRD results of chromium coatings with and without mPEG are shown in Fig. 7c. Peaks at 39.43, 44.36, and 48.88 were detected for chromium, indicating that Cr (200), Cr (210), and Cr (211) planes were deposited. The peaks at 42.01 and 72.15 for the Br-mPEG0 sample represent the brass foil substrate ($Cu_{0.64}Zn_{0.36}$). The detection of the brass substrate could result from a thin or cracked coating layer. Since the thickness of the Cr coatings from Br-mPEG0 (17 μm) and Br-mPEG80 (19 μm) are approximately the same, a cracked coating could be the main reason. As more cracks are formed during electrodeposition in Br-mPEG0 electrolyte (shown in Fig. 6a), the signal from the brass substrate is detected. Moreover, in aqueous chromium electrodeposition, additives can be co-deposited into the coating layer and form chromium carbides. However, elemental C and chromium carbide were not detected by EDS and XRD, indicating that this did not happen in the [BMIM]Br/H_2O system in this study.

4. CONCLUSIONS

The effect of mPEG in a mixed solution of ionic liquid and water was studied in this research with different concentrations of mPEG. The addition of mPEG significantly reduces the diffusion coefficient and increases the resistance of the electrolyte and charge transfer, resulting in a current decrease for both the chromium reduction reaction and HER. The concentration of H_2O molecules on the electrode surface decreases more than that of Cr(III) ions with 40 mmol L^{-1} mPEG in the electrolyte. Therefore, the amount of adsorbed Cr(III) ions is not reduced. With a further increase in mPEG concentration, the onset potential of Cr(III) reduction is negatively shifted. SEM images and corrosion tests prove that the decrease in electrodeposition rate caused by the addition of mPEG improves the surface morphology and corrosion resistance. However, with 100 mmol L^{-1} mPEG, pinholes are formed. Since the addition of mPEG prevents the HER and suppresses the formation of OH^-, more metallic Cr is deposited in the coating layer, as suggested by XPS and EDS. The optimum mPEG concentration studied here is 80 mmol L^{-1}. Our findings provide a promising strategy for using mPEG to achieve high-quality Cr(III) deposition.

ACKNOWLEDGEMENTS
This research was financially supported by the Collaborative Innovation Center for Petrochemical New Materials, Anqing, Anhui 246011, P.R. China (XTZX-2014-03), the Open Project of State Key Laboratory of Chemical Engineering (SKL-ChE-18C05), and the 111 Project of China (No. B08021).

References

1. L. Sziráki, E. Kuzmann, K. Papp, C. U. Chisholm, M. R. El-Sharif and K. Havancsák, *Mater. Chem. Phys.,* 133 (2012) 1092.
2. G. Saravanan and S. Mohan, *J. Appl. Electrochem.,* 39 (2009) 1393.
3. S. Survilienė, O. Nivinskienė, A. Češunienė and A. Selskis, *J. Appl. Electrochem.,* 36 (2006) 649.
4. Y. B. Song and D. T. Chin, *Electrochim. Acta,* 48 (2003) 349.
5. M. Aguilar-Sánchez, M. Palomar-Pardavé, M. Romero-Romo, M. T. Ramírez-Silva, E. Barrera and B. R. Scharifker, *J. Electroanal. Chem,* 647 (2010) 128.

6. J. Szynkarczuk, I. Drela and J. Kubicki, *Electrochim. Acta*, 34 (1989) 399.
7. D. Del Pianta, J. Frayret, C. Gleyzes, C. Cugnet, J. C. Dupin and I. Le Hecho, *Electrochim. Acta*, 284 (2018) 234.
8. M. Leimbach, C. Tschaar, U. Schmidt and A. Bund, *Electrochim. Acta*, 270 (2018) 104.
9. S. C. Kwon, M. Kim, S. U. Park, D. Y. Kim, D. Kim, K. S. Nam and Y. Choi, *Surf. Coat. Tech.*, 183 (2004) 151.
10. Y. Sheasha, D. Yücel, L. A. Kibler, M. Knape, S. Holl, S. Henne, S. Heitmüller and T. Jacob, *Chemelectrochem.*, 4 (2017) 1390.
11. M. Leng, S. Chen, J. Zhang, H. Lang, Y. Kang and S. Zhang, *Acta Chim. Sinica.*, 73 (2015) 403.
12. Y. Liu, Y. Ma, H. Yu and Y. An, *J. Chromatogr. Sci.*, 56 (2018) 1.
13. X. He, B. Hou, L. Chen, Q. Zhu, Y. Jiang and L. Wu, *Electrochim. Acta*, 130 (2014) 245.
14. L. Sun and J. F. Brennecke, *Ind. Eng. Chem. Res.*, 54 (2015) 4879.
15. S. Eugénio, C. M. Rangel, R. Vilar and S. Quaresma, *Electrochim. Acta*, 56 (2011) 10347.
16. B. Chen, J. Xu, L. Wang, L. Song and S. Wu, *ACS Appl. Mater. Interfaces.*, 9 (2017) 7793.
17. N. V. Phuong, S. C. Kwon, J. Y. Lee, J. H. Lee and K. H. Lee, *Surf. Coat. Tech.*, 206 (2012) 4349.
18. N. V. Phuong, S. C. Kwon, J. Y. Lee, J. Shin, B. T. Huy and Y. I. Lee, *Microchem. J.*, 99 (2011) 7.
19. M. Shamsipur, A. A. M. Beigi, M. Teymouri, S. M. Pourmortazavi and M. Irandoust, *J. Mol. Liq.*, 157 (2010) 43.
20. X. He, Q. Zhu, B. Hou, Y. Cai, C. Li, L. Fu and L. Wu, *J. Nanosci. Nanotechnol.*, 15 (2015) 9431.
21. L. E. T. Feliciano, A. J. A. D. Oliveira, W. H. Schreiner and E. C. Pereira, *J. Electroanal. Chem.*, 574 (2005) 333.
22. Protsenko V and Danilov F, *Electrochimica Acta*, 54 (2009) 5666.
23. A. M. A. Omar and E. M. S. Azzam, *Ind. Lub. Tribol.*, 56 (2013) 244.
24. A. Liang, N. I. Liwei, L. Qiao and J. Zhang, *Surf. Coat. Tech.*, 218 (2013) 23.
25. D. A. Johnson and M. A. Reid, *J. Electrochem. Soc.*, 132 (1985) 1058.
26. P. J. Elving and B. Zemel, *J. Am. Chem. Soc.*, 79 (1957) 1281.
27. C. Su, M. An, P. Yang, H. Gu and X. Guo, *Appl. Surf. Sci.*, 256 (2010) 4888.
28. N. Mohammadi, M. Najafi and N. B. Adeh, *Sensor. Actuat. B-Chem.*, 243 (2017) 838.
29. A. B. Steel, T. M. Herne and M. J. Tarlov, *Anal. Chem.*, 70 (1998) 4670.
30. Z. Min, M. Willey and A. C. West, *Electrochem. Solid ST.*, 8 (2005) 538.
31. L. Simanavičius, A. StakêNas and A. Šarkis, *Electrochim. Acta*, 42 (1997) 1581.
32. E. Michailova, I. Vitanova, D. Stoychev and A. Milchev, *Electrochim. Acta*, 38 (1993) 2455.
33. C. E. Lu, N. W. Pu, K. H. Hou, C. C. Tseng and M. D. Ger, *Appl. Surf. Sci.*, 282 (2013) 544.
34. Z. A. Hamid, *Surf. Coat. Tech.*, 203 (2009) 3442.